Environmental Science & Technology

Article

pubs.acs.org/est

Quantifying Contribution of Synthrophic Acetate Oxidation to Methane Production in Thermophilic Anaerobic Reactors by Membrane Inlet Mass Spectrometry

Daniel Girma Mulat,[†] Alastair James Ward,[†] Anders Peter S. Adamsen,[†] Niels Vinther Voigt,[‡] Jeppe Lund Nielsen,[§] and Anders Feilberg*[,†]

[†]Department of Engineering, Aarhus University, Hangøvej 2, DK-8200 Aarhus N, Denmark

[‡]Danish Technological Institute, Kongsvang Allé 29, DK-8000 Aarhus C, Denmark

[§]Center for Microbial Communities, Department of Biotechnology, Chemistry and Environmental Engineering, Aalborg University, Sohngaardsholmsvej 49, DK-9000 Aalborg, Denmark

Supporting Information

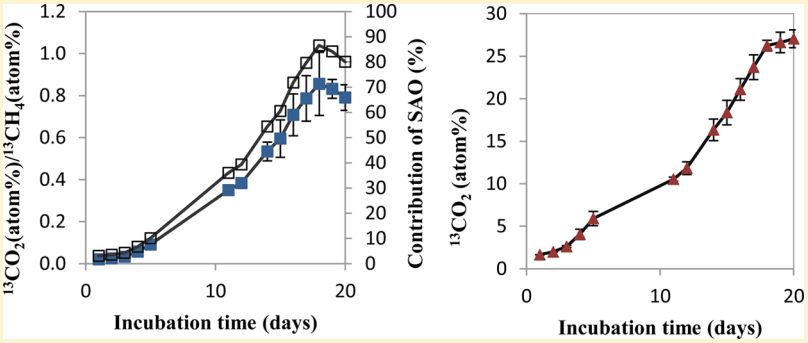

ABSTRACT: A unique method was developed and applied for monitoring methanogenesis pathways based on isotope labeled substrates combined with online membrane inlet quadrupole mass spectrometry (MIMS). In our study, a fermentation sample from a full-scale biogas plant fed with pig and cattle manure, maize silage, and deep litter was incubated with 100 mM of [2-^{13}C] sodium acetate under thermophilic anaerobic conditions. MIMS was used to measure the isotopic distribution of dissolved CO_2 and CH_4 during the degradation of acetate, while excluding interference from water by applying a cold trap. After 6 days of incubation, the proportion of methane derived from reduction of CO_2 had increased significantly and reached up to 87% of total methane, suggesting that synthrophic acetate oxidation coupled to hydrogenotrophic methanogenesis (SAO-HM) played an important role in the degradation of acetate. This study provided a new approach for online quantification of the relative contribution of methanogenesis pathways to methane production with a time resolution shorter than one minute. The observed contribution of SAO-HM to methane production under the tested conditions challenges the current widely accepted anaerobic digestion model (ADM1), which strongly emphasizes the importance of the acetoclastic methanogenesis.

1. INTRODUCTION

Acetate is a key intermediate in anaerobic digestion of organic matter, whereby it is converted to methane by two different pathways.[1−3] In acetoclastic methanogenesis (AM), acetate is directly cleaved in such a way that the methyl group of acetate is converted primarily to CH_4 while the carboxyl group is converted to CO_2 (Supporting Information (SI) Section 1). Acetate can also follow a two-step reaction pathway whereby acetate is first oxidized to CO_2 and H_2 by synthrophic acetate oxidation (SAO) and subsequently the CO_2 is reduced to CH_4 by hydrogenotrophic methanogenesis (HM) (SI Section 1). Under standard conditions, SAO is not thermodynamically favorable ($\Delta G^{\circ\prime}$ = +104.1 kJ/mol) and can only be feasible if the H_2 partial pressure is kept low by coupling with H_2-consuming methanogens.[3] It is generally assumed that acetoclastic methanogenesis is a dominant pathway for methane production from acetate. Therefore, biogas reactor operation and optimization is mostly based on maintaining favorable condition for acetoclastic methanogenesis, with little consideration to the importance of the SAO pathway. However, some studies recently found that SAO coupled to HM is a dominant pathway in thermophilic methanogenic reactors.[2−7] In most of the previous studies, the inoculum was sourced from anaerobic digesters treating sewage sludge[2,7] and synthetic wastewater.[6] The role of SAO-HM and its quantitative contribution to methane production in a mixed culture sourced from anaerobic digesters treating common agriculture wastes such as pig and

Received: January 15, 2014
Accepted: January 17, 2014
Published: January 17, 2014

cattle manure, maize silage, and deep litter manure is still unclear.

The relative contribution of methanogenesis pathways can be identified and quantified by measuring the isotopic distribution of CO_2 and CH_4[1,8] with gas chromatography−combustion−isotope ratio mass spectrometry (GC-C-IRMS)[9] and gas chromatography−mass spectrometry (GC-MS) in combination with ^{13}C labeled acetate.[2] In addition, radiometric measurement of $^{14}CH_4$ and $^{14}CO_2$ production is routinely employed to identify methanogenesis pathways with ^{14}C labeled substrates.[4] However, the offline gas sampling procedure in these techniques limits the knowledge on temporal variation of the isotopic distribution of CO_2 and CH_4. Moreover, the exact isotopic composition of dissolved gases in a liquid is not necessarily the same as that of gases in the headspace, since the latter is most probably modified by additional isotope effects during phase transition.[8]

Membrane inlet quadrupole mass spectrometry (MIMS) is an alternative technique to GC-MS, GC-C-IRMS, and radiometric approach for online measurement of the isotopic composition of dissolved CO_2 and CH_4 directly in a fermentation broth. Previous work has shown the suitability of MIMS based on a quadrupole analyzer for rapid detection of dissolved gases and volatile organic compounds in fermentation reactors[10−12] and specifically in a biogas process.[10,13,14] In addition to being simple, accurate, and fast, with response of seconds to minutes, MIMS is highly sensitive and does not require sample preparation.[12,14,15]

There have been only a few applications of MIMS for measuring isotopic distribution. One example is the measurement of the nitrogen isotopic distribution of N_2 gas with MIMS during incubation experiments after the addition of $^{15}NO_3^-$ tracer.[16] The MIMS method with ^{15}N isotope pairing was successfully applied for estimating the denitrification and nitrogen fixation simultaneously in aquatic systems.[17] Although the quadrupole mass spectrometry has a low resolution that limits its use for measuring isotopic distribution at natural abundance, it was demonstrated successfully for measuring the nitrogen isotopic distribution in conjunction with isotope pairing.[17] However, there has not been any report so far on its application for determining the carbon isotopic distribution of dissolved compounds in anaerobic reactors. To our knowledge, this is the first application of MIMS based on a quadrupole analyzer for monitoring the temporal variation in isotopic distribution of dissolved CH_4 and CO_2 in anaerobic digestion with ^{13}C labeled acetate.

In the present study, ^{13}C labeled acetate was used as a substrate in thermophilic anaerobic digestion and the incorporation of ^{13}C into CH_4 and CO_2 was monitored with MIMS. The source of the inoculum was a full-scale biogas digester working with a mixture of pig and cattle manure, maize silage, and deep litter manure. The aim of this study was two-fold. One aim was to investigate the capability of MIMS for monitoring the temporal variation in isotopic distribution of dissolved CH_4 and CO_2 in a fermentation broth. The second aim was to quantify the relative contribution of SAO-HM versus AM to methane production from high acetate concentration (100 mM) by following the temporal isotopic distribution of CH_4 and CO_2 with MIMS. Effects of temperature and cold trap were also investigated, which are important for optimization of the instrument. Moreover, we reported the linearity, response time, and detection limits of the MIMS methodology.

2. EXPERIMENTAL SECTION

Sources of Inoculum. Inoculum was obtained from a commercial full-scale biogas digester at research center Foulum, Denmark. The digester works with a mixture of pig and cattle manure, maize silage, and deep litter manure. It runs under thermophilic condition ca. 52 °C. The total solid (TS), volatile solid (VS), pH value, and total ammoniacal nitrogen (TAN) of the inoculum were 75.8 g/L, 60.6 g/L, 7.70, and 1.84 g/L, respectively. The inoculum was preincubated under anaerobic condition at 52 °C for 2 weeks prior to the main tracer experiment to reduce the background contribution of $^{12}CO_2$ and $^{12}CH_4$ from the original substrates.

Operation of Anaerobic Digestion. Glass serum bottles (500-mL) were used for preparing the anaerobic incubation assay. Aliquots (192 mL) of inoculum were transferred into the 500-mL serum bottles, which were then sealed with butyl rubber stoppers and aluminum crimps. Four treatments were prepared: (i) ^{13}C treatment with ^{13}C methyl labeled acetate, [2-^{13}C] sodium acetate, as the substrate, (ii) ^{13}C treatment with ^{13}C fully labeled acetate, [U-^{13}C] sodium acetate, as the substrate, (iii) unlabeled treatment with unlabeled sodium acetate as the substrate, and (iv) blank reactor with distilled water instead of substrate. The appropriate substrate was added once to each serum bottle to give a final concentration of 100 mM. Each ^{13}C treatment was run in duplicate, whereas unlabeled and blank treatments were run in quadruplicate under static incubation condition for 20 days at 52 °C.

MIMS Measurement. A schematic picture of the experimental setup for the MIMS measurement of the anaerobic incubation assay is presented in SI Figure S1.The MIMS system consisted of a quadrupole mass spectrometer (QMS) connected to a silicone membrane probe for the measurement of dissolved carbon dioxide and methane directly in a fermentation broth. Characteristic ions of each compound were monitored in multiple ion detection (MID) mode: m/z 17 for ^{13}C methane ($^{13}CH_4$), m/z 15 for ^{12}C methane ($^{12}CH_4$), m/z 45 for ^{13}C carbon dioxide ($^{13}CO_2$), m/z 44 for ^{12}C carbon dioxide ($^{12}CO_2$) and m/z 18 for water (H_2O). A dry ice cold trap was used in the vacuum line to minimize interference of water on methane measurements.[18] Two types of MIMS measurements were employed:

(i) MIMS measurement of standard solution: Aqueous standard solutions of carbon dioxide and methane at different concentrations were prepared from a standard gas mixture of CO_2 and CH_4. The dissolved concentration of methane and carbon dioxide in water was calculated from the product of gas partial pressure and temperature-corrected Henry's constants.[19] The temperature-corrected Henry's constants (k_H) for CH_4 and CO_2 at 52 °C are 0.00225 and 0.0663 M/atm, respectively, which were calculated from the Henry's constants at standard condition (k^o_H), the temperature dependence of the Henry's constants and the actual temperature of the incubation experiment.[19]

(ii) MIMS measurement of anaerobic digestion: MIMS measurement was carried out for duplicate experiments for all of the four treatments, giving a total of eight reactors to be measured every day. Because the MIMS system was equipped with only one membrane probe, the MIMS probe was switched among the eight reactors and the MIMS measurement was conducted for 4 min in each reactor. To sum up, the MIMS measurements of

eight reactors were conducted every 4 min for the total of 20 incubation days. The details of the MIMS setup are given in SI Section 2.

Analytical Methods and Proteome Analysis. Gas composition (CO_2 and CH_4) and volume were measured periodically. The concentrations of VFAs and pH were measured almost every day. Liquid samples for proteome analysis were collected from all reactors at the middle of the incubation experiment. A detail description of the method is provided in SI Section 2.

Calculation of Isotope Distribution. The proportion of $^{12}CO_2$, $^{13}CO_2$, $^{12}CH_4$, and $^{13}CH_4$ during the degradation of [2-^{13}C]acetate depends on the methanogenesis pathways (SAO-HM and AM). Moreover, the proportion of $^{13}CH_4$ and $^{12}CH_4$ during SAO-HM pathway is affected by the kinetic isotope effect, whereby the production of $^{12}CH_4$ is slightly faster than $^{13}CH_4$ during the reduction of $^{12}CO_2$ and $^{13}CO_2$, respectively (i.e., $^{12}k/^{13}k$ = 1.065 on average under thermophilic condition).[8,20]

The proportion of $^{13}CO_2$ to total carbon dioxide, $^{13}CO_2$ (atom%), indicates the contribution level of SAO pathway to methane production due to the fact that $^{13}CO_2$ will be produced only via SAO oxidation of $^{13}CH_3COO^-$ (SI eq S2). On the other hand, a significant proportion of $^{13}CH_4$ to total methane will be produced if $^{13}CH_3COO^-$ is directly cleaved by AM (SI eq S1). Hence, the proportion of $^{13}CH_4$ to total methane production, $^{13}CH_4$ (atom%), during the degradation of $^{13}CH_3COO^-$ ascribed to the contribution of AM to methane production. Therefore, the contribution (%) that SAO coupled to HM makes to total methane production can be expressed in terms of the ratio of $^{13}CO_2$ (atom%) to $^{13}CH_4$ (atom%). An increase in the ratio of $^{13}CO_2$ (atom%) to $^{13}CH_4$ (atom%) represents the increase in the contribution of SAO-HM to methane production and vice versa. The terms "SAO-HM" and "SAO" are used interchangeably in our study when describing the quantitative contribution of SAO pathway to methane production.

An example of a schematic representation of calculated mass balance of $^{13}CH_4$, $^{12}CH_4$, $^{13}CO_2$, and $^{12}CO_2$ by assuming 50% methane production from acetoclastic methanogenesis and the remaining 50% from SAO is shown in Figure S2 (SI Section 2). The kinetics isotope effect during the reduction of carbon dioxide to methane, $^{12}k/^{13}k$ = 1.065,[8,20] was included in the calculation. Using this principle, the mass balance of each carbon isotope species assuming 0% up to 100% SAO pathway was calculated. In Figure 1, the quantitative contribution of SAO (%) to methane production is shown as a function of the calculated ratio of atom% of $^{13}CO_2$ to $^{13}CH_4$, which was linear. The linear equation obtained in Figure 1 was rewritten as eq 1 to estimate the contribution of SAO to methane production as a function of $^{13}CO_2$ (atom%)/$^{13}CH_4$ (atom%). The overall uncertainty associated with estimation of SAO (%) using eq 1 as a function of MIMS data of $^{13}CO_2$ (atom%)/$^{13}CH_4$ (atom%) was 5.9% (SI Section 7).

$$\mathrm{SAO}(\%) = \frac{y + 0.01}{0.01} \quad (1)$$

where y is $^{13}CO_2$ (atom%)/$^{13}CH_4$ (atom%).

Experimental Methods for the Quantification of SAO-HM Pathway Using MIMS Data. In our study, MIMS was used to measure the isotopic distribution of dissolved carbon dioxide ($^{12}CO_2$ and $^{13}CO_2$) and methane ($^{12}CH_4$ and $^{13}CH_4$) during the anaerobic digestion of [2-^{13}C]acetate and [U−^{13}C]-acetate. The [2-^{13}C]acetate substrate was used to study methanogenesis pathways. On the other hand, the [U−^{13}C]-acetate substrate was used to correct the background total inorganic carbon (TIC) arising from the inoculum. The unlabeled products ($^{12}CO_2$ and $^{12}CH_4$) during the degradation of [U−^{13}C]acetate were considered as the background TIC that comes from the inoculum and they were subtracted from the MIMS values of $^{12}CO_2$ and $^{12}CH_4$ measured during the degradation of [2-^{13}C]acetate. The background TIC was accounted in this way for reporting the TIC-corrected $^{13}CO_2$ (atom%)/$^{13}CH_4$ (atom%) of [2-^{13}C]acetate reactor. The quantitative contribution (%) that SAO makes to total methane production was determined by solving eq 1 with the TIC-corrected $^{13}CO_2$ (atom%)/$^{13}CH_4$ (atom%) of [2-^{13}C]acetate reactor. The details of MIMS data presentation is described in SI Section 2.

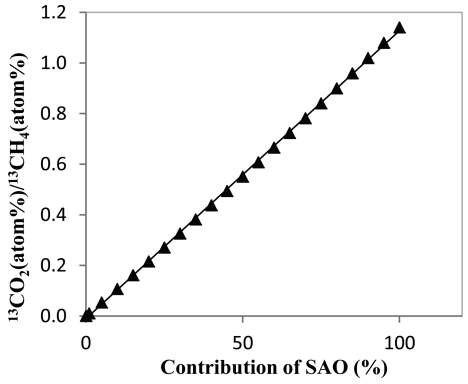

Figure 1. Quantitative contribution of SAO (%) to methane production as a function of the calculated ratio of atom% of $^{13}CO_2$ to $^{13}CH_4$.

3. RESULTS AND DISCUSSION

Characteristic Performance of MIMS for CO_2 and CH_4 Measurement. With our constructed anaerobic reactor and application of the cold trap, dissolved CO_2 and CH_4 were directly measured by MIMS without interference from water. The cold trap not only effectively condensed the water vapor that otherwise interferes with the measurement of $^{13}CH_4$ (SI Figure S3), but it also reduced the pressure inside the mass spectrometer (data not shown). Tests of the effect of sample temperature on the MIMS instrument showed that safe operation of a MIMS system is achievable for typical anaerobic digestion temperatures (30−52 °C). It is important to maintain a constant sample temperature while measuring dissolved CO_2 and CH_4 with MIMS; otherwise the temperature difference leads to different signal intensities (SI Figure S4). The response time of the instrument was faster than 1 min for both CH_4 and CO_2 (SI Figure S5). The observed fast response time showed that MIMS can be used for online and onsite measurements of dissolved carbon dioxide and methane in real time.

External Standard Calibration and Detection Limit. Standard solutions of methane and carbon dioxide were prepared by continuously purging a standard gas mixture through deionized water until equilibrium concentrations were reached. Calibration curves were obtained by plotting the peak area of standard solutions versus the known concentrations of the dissolved gases. Although the cold trap was an effective means for condensing the water vapor that otherwise interferes

dx.doi.org/10.1021/es403144e | Environ. Sci. Technol. 2014, 48, 2505−2511

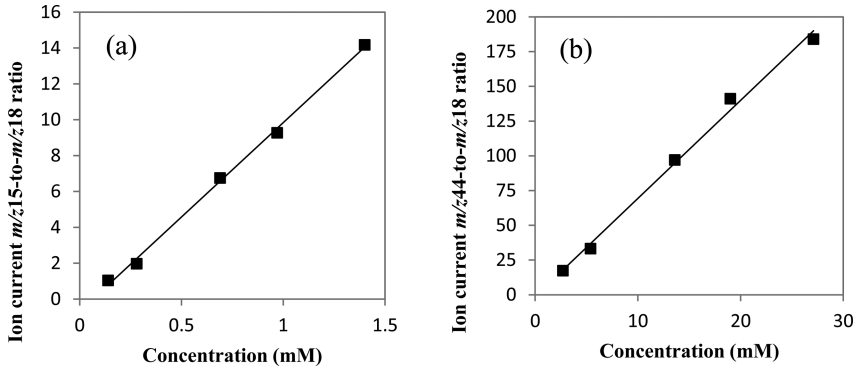

Figure 2. Calibration curves for (a) methane (ion current m/z 15 to m/z 18 ratio) and (b) carbon dioxide (ion current m/z 44 to m/z 18 ratio) using MIMS.

with the measurement of $^{13}CH_4$, the diffusion of a small amount of water into the mass spectrometry is unavoidable. The presence of water in the mass spectrometry affects the intensity of the ions measured by the MIMS. Therefore, the absolute intensities were normalized with the intensity of m/z 18 (H_2O^+) to obtain comparable data. All the intensities presented in the manuscript are relative (normalized) intensities (Figures 2 and SI S6). Dissolved carbon dioxide and methane showed a linear dynamic range in the concentration range of 2.7−27.1 mM (r^2 = 0.994) and 0.14−1.4 mM (r^2 = 0.998), respectively (Figure 2). The detection limits of CO_2 and CH_4 (calculated from three times the standard deviation of the replicate blank samples) were 0.07 and 0.28 mM, respectively. By implementing the cold trap, the detection limit of CH_4 was improved by a factor of 3 (from 0.84 to 0.28 mM) due to the reduction of the pressure inside the mass spectrometer.

Degradation of Acetate and Methane Production. In our experiment, a small concentration of acetate was detected in the blank (inoculum only) reactors (less than 5 mM and estimated to be less than 5% of the added acetate in the other reactors). The methane production from the blank reactor was very small (less than 5% of the acetate-fed reactors). The methane production of ^{13}C labeled reactors was corrected for the methane produced by the inoculum. The accumulated methane production for the [2-^{13}C]acetate reactor was 234.7 mL/g COD and variations in methane production for the duplicate assays were less than (±3.5) mL/g COD, which is very small (Figure 3). In addition, acetate degradation also exhibited very small variation (±1 to ±4 mM) for the first 14 days for the duplicate assays (Figure 3). The last 6 days of the incubation period showed slightly higher variation of acetate degradation (±5 to ±6 mM) for the duplicate assays.

Methane production from degradation of 100 mM [2-^{13}C]-acetate followed a typical batch experiment whereby methane production rate was slower at the beginning of the incubation, followed by exponential increase of methane production and a later stationary phase (Figure 3). It is clear from Figure 3 that both acetate degradation and accumulated methane production showed similar patterns for the whole incubation period. The acetate degradation was very slow in the first 6 days of the incubation except for the first 48 h (Figure 3). Acetate concentration was reduced by 8 mM and methane production was increased by 20 mL/g COD in the first 48 h. The reason for the high acetate degradation rate for 48 h followed by a slower degradation rate from day 3 until day 6 was apparently unknown. However, the slow acetate degradation rate from day

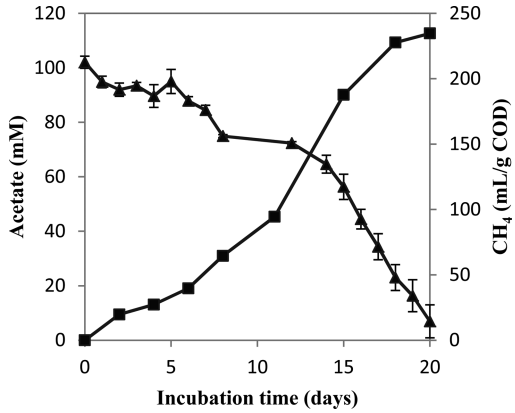

Figure 3. Temporal change in the degradation of 100 mM [2-^{13}C]acetate (▲) and accumulated methane production (■) from 100 mM [2-^{13}C]acetate. The lines represent mean values (n = 2) and error bars denote the data range.

3 until day 6 and a subsequent increase in acetate degradation rate afterward until day 18 is a typical lag phase for this type of reactor (Figure 3). A decrease in acetate concentration from 88 to 23 mM from day 6 until day 18 was accompanied by a significant increase in methane production from 40 to 288 mL/g COD (Figure 3). Almost 72% of acetate was degraded during this period. When the acetate concentration was less than 23 mM on the last 2 days of the incubation, the accumulated methane production was reduced slightly (Figure 3).

Estimation of Methanogenic Pathways to Total Methane Production from [2-^{13}C]Acetate. The evolution of $^{13}CH_4$, $^{12}CH_4$, $^{12}CO_2$, and $^{13}CO_2$ during the degradation of [2-^{13}C]acetate was followed using the developed MIMS method. The contribution of the background total inorganic carbon (TIC) from the inoculum was corrected from the measured [2-^{13}C]acetate incubation and the TIC-corrected MIMS data are presented as $^{13}CO_2$ (atom%)/$^{13}CH_4$ (atom%) (Figure 4a) and $^{13}CO_2$ (atom%) (Figure 4b). The ratio of TIC-corrected $^{13}CO_2$ (atom%) to $^{13}CH_4$ (atom%) was used to estimate the contribution of SAO-HM pathway to methane production according to eq 1 and it is shown in Figure 4a.

The proportion of $^{13}CO_2$ to total carbon dioxide, represented as $^{13}CO_2$ (atom%), is a clear qualitative demonstration of the SAO pathway. The evolution of the higher amount of $^{13}CO_2$ compared to total carbon dioxide production can only happen due to continuous production of $^{13}CO_2$ from [2-^{13}C]acetate by SAO according to SI equation S2. Therefore, the observed increase in $^{13}CO_2$ (atom%) is a qualitative indication of the

dx.doi.org/10.1021/es403144e | Environ. Sci. Technol. 2014, 48, 2505−2511

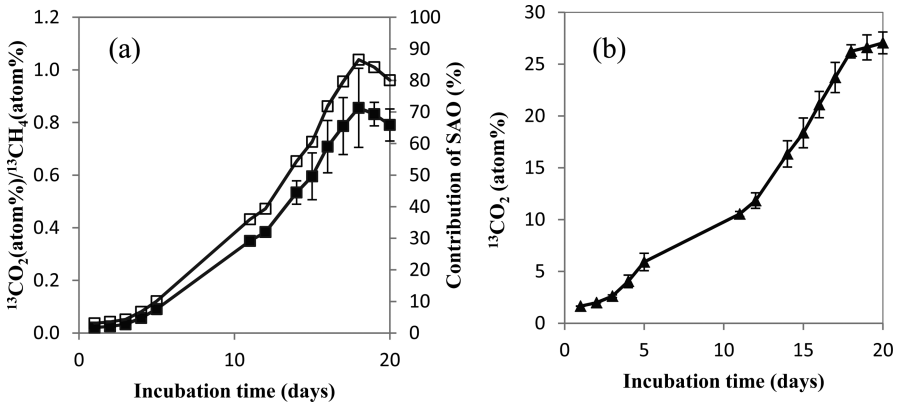

Figure 4. Temporal evolution of (a) $^{13}CO_2$ (atom%)/$^{13}CH_4$ (atom%) (■) and the contribution of SAO (%) to methane production (□); (b) $^{13}CO_2$ (atom%) (▲). The lines represent mean values (n = 2) and error bars denote the data range.

increase in contribution of SAO to acetate degradation over time (Figure 4b). The subsequent discussion is an attempt to quantify the contribution (%) of SAO-HM during the degradation of acetate to methane.

In Figure 4a and b the temporal evolution of the ratio of $^{13}CO_2$ (atom%) to $^{13}CH_4$ (atom%) and $^{13}CO_2$ (atom%) followed three distinct trends which can be roughly grouped according to the incubation time (the first 5 days, day 11−18, and the last 2 days). MIMS measurement from day 6 until day 10 was not conducted due to the failure of the instrument to maintain the required high vacuum (~10^{-6} mbar). MIMS measurement was resumed on day 11 after the leak was repaired.

A very small change in the proportion of $^{13}CO_2$ (atom%) from 1.7 to 5.9 was observed during the first 5 days of the incubation period (Figure 4b). Similar to the change in $^{13}CO_2$ (atom%), the change in the ratio of $^{13}CO_2$ (atom%) to $^{13}CH_4$ (atom%) was very slow (Figure 4a), i.e. it changes from 0.02 to 0.09. The calculated contributions (%) of SAO-HM to total methane production range from 3% to 10% (Figure 4a). This small contribution of SAO-HM corroborates well with the slow methane production rate and acetate degradation rate during the first 6 days of the incubation period (Figure 3).

As shown from TIC-corrected MIMS data for day 5 to 11, the proportion of $^{13}CO_2$ (atom%) was increased from 5.9 to 10.5 (Figure 4b) and subsequently the ratio of $^{13}CO_2$ (atom%) to $^{13}CH_4$ (atom%) was increased from 0.09 to 0.35 (Figure 4a). The contribution of SAO-HM to methane production was increased by 26% from day 5 to 11 (Figure 4a). Although we missed the MIMS measurement from day 6 until day 10, it is obvious that SAO-HM is taking place at a higher rate as shown from MIMS data on days 5 and 11. Accumulated methane production was also increased by 54.7 mL/g COD and acetate was reduced by 23 mM between day 6 and 11 (Figure 3).

The ratio of $^{13}CO_2$ to total carbon dioxide was increased significantly from 10.5 to 26.2 atom % from day 11 to 18 (Figure 4b). Similarly, the ratio of $^{13}CO_2$ (atom%) to $^{13}CH_4$ (atom%) was increased significantly from 0.35 to 0.86 (Figure 4a). The SAO-HM contribution to methane production was increased from 36 to 87% of the methane production in this period (Figure 4a). The increase in SAO-HM over time showed that there is a shift of methanogenic pathways from acetoclastic methanogenesis to SAO-HM pathways during the course of the incubation of [2-^{13}C]acetate. Accumulated methane production was increased significantly by 133.3 mL/g COD and acetate was reduced by 49 mM from day 11 until day 18 (Figure 3). The shift in methanogenic pathway was accompanied by faster acetate degradation and high methane production rate.

The evolution rate of $^{13}CO_2$ to total carbon dioxide was slightly slower in the last 2 days of the incubation and remained at 27.1 atom% (Figure 4b). Similarly, the ratio of $^{13}CO_2$ (atom %) to $^{13}CH_4$ (atom%) had started to decrease slightly and reached 0.79 (Figure 4a). As shown in Figure 3, the methane production rate decreased as a consequence of the small concentration of acetate available in the reactor (Figure 3). The slight decrease in the ratio of $^{13}CO_2$ (atom%) to $^{13}CH_4$ (atom %) could be attributed to a decrease in production of carbon dioxide derived from the oxidation of acetate at low acetate concentration. Despite the decrease in the ratio, SAO-HM was still the dominant acetate degradation pathway, which contributed up to 80% of the methane production from acetate even in the presence of a small concentration of acetate. Both acetoclastic methanogenesis and SAO-HM contributed to the degradation of acetate at different proportion and the contribution of the latter was increased during the course of the incubation. All in all, the SAO-HM contributed to 49% of the total methane production (147 mL of methane out of the total 300 mL of methane) whereas the remaining 51% of the total methane (153 mL of methane) was produced via the acetoclastic methanogenesis.

Microbial Community Composition. The microbial community composition were analyzed by using a proteome analysis and revealed a heterogeneous distribution representing 18 phyla, 30 classes, and 107 genera. Bacterial proteins represented 74.5% of the proteins, while archaeal proteins accounted for most of the remaining (~25%). The most abundant phyla were *Firmicutes* (30.9%), *Euryarchaeota* (23.3%), *Proteobacteria* (16.5%), and *Bacteroidetes* (5.7%), while the most abundant classes were *Methanomicrobia* (23%), *Clostridia* (19.7%), and *Bacilli* (8%) (SI Table S2). Within the *Archaea*, the mixotrophic *Methanosarcina* (10.8%) and hydrogenotrophic *Methanoculleus* (8.7%) were the most abundant methanogens. *Methanoculleus sp.* and *Methanosarcina sp.* have been reported as widely distributed in thermophilic anaerobic reactors, especially those treating manure and agricultural wastes.[21,22] Similar diversity of *Bacteria* and *Archaea* communities were present in all acetate-fed and blank reactors (data not shown).

Merits of MIMS Measurement. In our study, the MIMS probe was submerged in a fermentation broth and the MIMS measurement was taken for few minutes. The MIMS probe was

dx.doi.org/10.1021/es403144e | *Environ. Sci. Technol.* 2014, 48, 2505−2511

not submerged in one sample for the whole incubation period (20 days), since only one membrane probe was available and there was a need to run many samples per day. In some cases, MIMS probe multiplexing can be used to continuously measure dissolved gases in several fermentors whereby multiple membrane probes are coupled to one quadruple mass spectrometer (QMS) through sufficiently long vacuum pipelines and a multivalve system.[11] Hence, it is more a demonstration of the principle, which can be used for online and continuous monitoring in one or several reactors if multiple membrane probes that work with high vacuum system are constructed.

In previous studies where GC-MS was used in combination with ^{13}C labeled substrates, the headspace gas samples were measured offline once usually at the end of the incubation.[2,23] Consequently, the quantitative contribution of each methanogenetic pathway to methane production during the incubation period, where acetate concentration changed significantly, was not provided. This study, however, provided a new approach for online quantification of the relative contribution of methanogenesis pathways to methane production with a time resolution of shorter than 1 minute. This shorter time resolution and continuous isotope measurement demonstrated that an increase in the proportion of SAO-HM to methane production was accompanied with a rapid acetate degradation and high methane production rate in the study presented here. Another disadvantage of the headspace gas measurement by GC-MS is that the isotopic composition of the headspace gas is not necessarily the same as the dissolved gas, since the former is most probably modified by additional isotope effects during phase transition.[8] In this study, however, MIMS was applied for rapidly monitoring the isotopic distribution of dissolved gases in a liquid.

There are also inconsistencies in the way GC-MS data were used to quantify the contribution (%) of SAO to methane production. For instance, Hori et al.[23] reported the proportion of methane produced via SAO pathway was equal to the value of atom% of $^{13}CH_4$ whereas Sasaki et al.[2] multiplied the value of atom% of $^{13}CH_4$ by 2 to calculate the contribution of SAO (%) to total methane production. In our study, however, the calculation of the isotopic distribution of carbon dioxide and methane was thoroughly executed and the kinetic isotope effect was also included in the calculation. The mathematical equation (eq 1) we derived from the isotopic calculation was shown to provide a good estimation to the quantitative contribution of SAO pathway to methane production.

With regard to the established ^{14}C radioisotope tracer experiment, only qualitative information can be obtained in order to identify which pathway dominates the degradation of acetate. In radioisotope analysis, if $^{14}CO_2/^{14}CH_4 > 1$, SAO is judged to be a dominant pathway during the degradation of [2-^{14}C]acetate, otherwise acetoclastic methanogenesis predominates.[4] There are also several difficulties working with radioisotope tracer experiments because of the requirement for strict health and safety regulations for handing radioisotopes, and high cost associated radioactive material training, regulation, and waste disposal.[24]

SAO As a Key Acetate Degradation Pathway. In this study, it has been shown that synthrophic acetate oxidation coupled to hydrogenotrophic methanogenesis is an important methanogenic pathway which contributes from 3% to 87% of methane production on average during the course of acetate degradation. Similar findings were reported in a few studies, where SAO contributed 35−89%,[7] 80%,[2] and 13.1−21.3%.[23] The difference in the contribution level of SAO to methane production may originate in the source of inoculum and concentration of acetate used as a substrate. For instance, 100 mM[7] and 4 mM[2] acetate were inoculated with mixed cultures obtained from anaerobic digesters treating sewage sludge, and 0.5 mM acetate[23] was inoculated with a mixed culture obtained from an anaerobic digester treating synthetic wastewater. The findings from previous studies[2,7,23] and our study indicate that SAO is favored at high acetate concentration (4−100 mM). However, further research is required to understand the role of SAO at different environmental conditions such as acetate concentration, ammonia, inoculum sources, and temperature.

Analysis of the community structure of the thermophilic anaerobic digester sludge showed that methane production was stable and efficient without acetate accumulation even in the absence of strict acetoclastic methanogens (*Methanosaetaceae*). The digesters were dominated by synthrophic acetate oxidizing bacteria (SAOB) in synthrophic association with strict hydrogenotrophic methanogens (often *Methanobacteriales* or *Methanomicrobiales*).[4] Abundant synthrophic acetate oxidizing bacteria affiliate into the class *Clostridia* within the phylum *Firmicutes* as well as the family *Thermotogaceae* within the phylum *Thermotogae*.[3] In our study, it appears that bacteria belonging to the phyla *Firmicutes* are those mainly responsible for acetate oxidation with a subsequent methane production by the hydrogenotrophic *Methanoculleus*. Moreover, species within the mixotrophic *Methanosarcinaceae* able to utilize several substrates such as acetate, hydrogen and carbon dioxide, methanol, and methylamines were also prevalent in the digesters.[4,25] Given their ability to shift between the two metabolisms depending on growth conditions[26] and being a mixotrophic microorganism, members of the *Methanosarcina* may play an important role for the conversion of acetate to methane via both acetoclastic and synthrophic acetate oxidation coupled to hydrogenotrophic methanogenesis in the study presented here.

Microorganisms mediating SAO-HM pathway have shown to tolerate environmental stress such as high organic loading and high levels of ammonium up to 7000 mg TAN/L.[5,27] Further experiments into the role of SAO-HM pathways could open a new possibility to optimize biogas production by maintaining favorable environmental condition for these stress-tolerant microorganisms. Moreover, kinetic parameters will be required in order to modify the currently widely accepted anaerobic digestion model (ADM1) which emphasizes acetoclastic methanogenesis as a dominant pathway of methane production from acetate.[28] In this regard, the rapid and simple technique employed in our study can be used in future experiments to facilitate the insight into the kinetics and quantitative information of SAO-HM pathway to methane production.

■ ASSOCIATED CONTENT

Ⓢ Supporting Information

Acetate degradation reactions, details of experimental part, additional results, and other details. This information is available free of charge via the Internet at http://pubs.acs.org/.

■ AUTHOR INFORMATION

Corresponding Author

*Phone: +45 30896099; e-mail: af@eng.au.dk.

Notes

The authors declare no competing financial interest.

■ ACKNOWLEDGMENTS

This research was financially supported by the Danish Strategic Research Council (Grant 10-093944).

■ REFERENCES

(1) Zinder, S. H.; Koch, M. Non-aceticlastic methanogenesis from acetate: Acetate oxidation by a thermophilic syntrophic coculture. *Arch. Microbiol.* **1984**, *138*, 263−272.
(2) Sasaki, D.; Hori, T.; Haruta, S.; Ueno, Y.; Ishii, M.; Igarashi, Y. Methanogenic pathway and community structure in a thermophilic anaerobic digestion process of organic solid waste. *J. Biosci. Bioeng.* **2011**, *111*, 41−46.
(3) Hattori, S. Syntrophic acetate-oxidizing microbes in methanogenic environments. *Microbes Environ.* **2008**, *23*, 118−127.
(4) Karakashev, D.; Batstone, D. J.; Trably, E.; Angelidaki, I. Acetate oxidation is the dominant methanogenic pathway from acetate in the absence of Methanosaetaceae. *Appl. Environ. Microbiol.* **2006**, *72*, 5138−5141.
(5) De Vrieze, J.; Hennebel, T.; Boon, N.; Verstraete, W. Methanosarchina: The rediscovered methanogen for heavy duty biomethanation. *Bioresour. Technol.* **2012**, *112*, 1−9.
(6) Hori, T.; Haruta, S.; Ueno, Y.; Ishii, M.; Igarashi, Y. Dynamic transition of a methanogenic population in response to the concentration of volatile fatty acids in a thermophilic anaerobic digester. *Appl. Environ. Microbiol.* **2006**, *72*, 1623−1630.
(7) Hao, L. P.; Lü, F.; He, P. J.; Li, L.; Shao, L. M. Predominant contribution of syntrophic acetate oxidation to thermophilic methane formation at high acetate concentrations. *Environ. Sci. Technol.* **2010**, *45*, 508−513.
(8) Conrad, R. Quantification of methanogenic pathways using stable carbon isotopic signatures: A review and a proposal. *Org. Geochem.* **2005**, *36*, 739−752.
(9) Meier-Augenstein, W. Applied gas chromatography coupled to isotope ratio mass spectrometry. *J. Chromatogr. A* **1999**, *842*, 351−371.
(10) Lloyd, D.; Bohátka, S.; Szilágyi, J. Quadrupole mass-spectrometery in the monitoring and control of fermentations. *Biosensors* **1985**, *1*, 179−212.
(11) Bohátka, S. Process monitoring in fermentors and living plants by membrane inlet mass spectrometry. *Rapid Commun. Mass Spectrom.* **1997**, *11*, 656−661.
(12) Tarkiainen, V.; Kotiaho, T.; Mattila, I.; Virkajarvi, L.; Aristidou, A.; Ketola, R. A. On-line monitoring of continuous beer fermentation process using automatic membrane inlet mass spectrometric system. *Talanta* **2005**, *65*, 1254−1263.
(13) Ward, A. J.; Bruni, E.; Lykkegaard, M. K.; Feilberg, A.; Adamsen, A. P. S.; Jensen, A. P.; Poulsen, A. K. Real time monitoring of a biogas digester with gas chromatography, near-infrared spectroscopy, and membrane-inlet mass spectrometry. *Bioresour. Technol.* **2011**, *102*, 4098−4103.
(14) Bastidas-Oyanedel, J.-R.; Mohd-Zaki, Z.; Pratt, S.; Steyer, J.-P.; Batstone, D. J. Development of membrane inlet mass spectrometry for examination of fermentation processes. *Talanta* **2010**, *83*, 482−492.
(15) Davey, N. G.; Krogh, E. T.; Gill, C. G. Membrane-introduction mass spectrometry (MIMS). *TrAC, Trends Anal. Chem.* **2011**, *30*, 1477−1485.
(16) An, S.; Gardner, W. S.; Kana, T. Simultaneous measurement of denitrification and nitrogen fixation using isotope pairing with membrane inlet mass spectrometry analysis. *Appl. Environ. Microbiol.* **2001**, *67*, 1171−1178.
(17) Steingruber, S. M.; Friedrich, J.; Gächter, R.; Wehrli, B. Measurement of denitrification in sediments with the 15N isotope pairing technique. *Appl. Environ. Microbiol.* **2001**, *67*, 3771−3778.
(18) Schlüter, M.; Gentz, T. Application of membrane inlet mass spectrometry for online and in situ analysis of methane in aquatic environments. *J. Am. Soc. Mass Spectrom.* **2008**, *19*, 1395−1402.
(19) Sander, R. *Compilation of Henry's Law Constants for Inorganic and Organic Species of Potential Importance in Environmental Chemistry*; Max-Planck Institute of Chemistry, Air Chemistry Department: Mainz, Germany, 1999; pp 1−107.
(20) Pohlman, J.; Kaneko, M.; Heuer, V.; Coffin, R.; Whiticar, M. Methane sources and production in the northern Cascadia margin gas hydrate system. *Earth Planet. Sci. Lett.* **2009**, *287*, 504−512.
(21) Demirel, B.; Scherer, P. The roles of acetotrophic and hydrogenotrophic methanogens during anaerobic conversion of biomass to methane: A review. *Rev. Environ. Sci. Biotechnol.* **2008**, *7*, 173−190.
(22) Kröber, M.; Bekel, T.; Diaz, N. N.; Goesmann, A.; Jaenicke, S.; Krause, L.; Miller, D.; Runte, K. J.; Viehöver, P.; Pühler, A. Phylogenetic characterization of a biogas plant microbial community integrating clone library 16S-rDNA sequences and metagenome sequence data obtained by 454-pyrosequencing. *J. Biotechnol.* **2009**, *142*, 38−49.
(23) Hori, T.; Sasaki, D.; Haruta, S.; Shigematsu, T.; Ueno, Y.; Ishii, M.; Igarashi, Y. Detection of active, potentially acetate-oxidizing syntrophs in an anaerobic digester by flux measurement and formyltetrahydrofolate synthetase (FTHFS) expression profiling. *Microbiology* **2011**, *157*, 1980−1989.
(24) Pack, M. A.; Heintz, M. B.; Reeburgh, W. S.; Trumbore, S. E.; Valentine, D. L.; Xu, X.; Druffel, E. R. A method for measuring methane oxidation rates using low-levels of 14C-labeled methane and accelerator mass spectrometry. *Limnol. Oceanogr.-Methods* **2011**, *9*, 245−260.
(25) Krakat, N.; Westphal, A.; Schmidt, S.; Scherer, P. Anaerobic digestion of renewable biomass: Thermophilic temperature governs methanogen population dynamics. *Appl. Environ. Microbiol.* **2010**, *76*, 1842−1850.
(26) Qu, X.; Mazeas, L.; Vavilin, V. A.; Epissard, J.; Lemunier, M.; Mouchel, J. M.; He, P. j.; Bouchez, T. Combined monitoring of changes in $\delta^{13}CH_4$ and archaeal community structure during mesophilic methanization of municipal solid waste. *FEMS Microbiol. Ecol.* **2009**, *68*, 236−245.
(27) Schnürer, A.; Nordberg, A. Ammonia, a selective agent for methane production by syntrophic acetate oxidation at mesophilic temperature. *Water Sci. Technol.* **2008**, *57*, 735−740.
(28) Batstone, D. J.; Kelle, J.; Steyer, J. A review of ADM1 extensions, applications, and analysis: 2002−2005. *Water Sci. Technol.* **2006**, *54*, 1−10.